

Quenched Chiral Corrections to Heavy-Light Decay Constants at Order $1/M$

Michael J. Booth

Institute for Fundamental Theory and Department of Physics
University of Florida, Gainesville, Florida 32611
booth@phys.ufl.edu

ABSTRACT

Quenched chiral perturbation is used to study the decay constants for heavy-light mesons beyond the leading order in $1/M$. The results are used to estimate the error in quenched lattice calculations of the decay constants. For the double ratio $R_1 = (f_{D_s}/f_D)/(f_{B_s}/f_B)$ we find that the error is small — conservatively 5%, but likely smaller. We also find that quenching decreases the ratio f_{D_s}/f_D relative to the unquenched theory.

PACS: 12.38.Gc, 12.39.Fe, 12.39.Hg

1 Introduction

The decay constants of the heavy-light mesons (B and D families) play a leading role in the physics of those mesons. In particular, $B\bar{B}$ mixing is proportional to f_B^2 . Thus, knowledge of f_B is important for estimates of mixing rate and the extraction of the CKM angles. Consider the experimental quantity

$$R_2 = \frac{(\Delta M/\Gamma)_{B_s}}{(\Delta M/\Gamma)_B}. \quad (1)$$

To a good approximation,

$$R_2 = \left| \frac{V_{ts}}{V_{td}} \right|^2 \left(\frac{f_{B_s}}{f_B} \right)^2 \frac{B_{B_s}}{B_B}. \quad (2)$$

However, in order for this to provide a meaningful determination of $|V_{ts}/V_{td}|$, the ratios f_{B_s}/f_B and B_{B_s}/B_B must be known precisely. They have been studied within heavy meson chiral perturbation theory (HChPT)[1, 2, 3, 4] with the result that B_{B_s}/B_B is close to unity, while f_{B_s}/f_B is about 1.2. The large deviation from unity of this latter quantity casts doubt on the reliability of HChPT. Because of this Grinstein[3] has advocated using instead $R_1 \times f_{D_s}/f_D$, where

$$R_1 = \frac{f_{B_s}}{f_B} / \frac{f_{D_s}}{f_D}. \quad (3)$$

and f_{D_s}/f_D is taken from experiment.

The advantage of this approach is that the ratio R_1 is sensitive only to corrections which violate *both* heavy quark and chiral symmetries. From the point of view of the heavy quark effective theory, this may be obvious, but it is nonetheless worth emphasising the idea behind it, which is simply that the long distance physics described by the chiral theory is insensitive to the actual mass of the heavy quark. Thus, one expects that while the chiral corrections may be badly behaved, their variation with respect to M (probed by R_1) should be under control. Indeed, this expectation was born-out in a recent calculation by Boyd and Grinstein[4] (BG) which found that R_1 differs from unity by only -5% .

The properties of heavy mesons have also been studied intently on the lattice. In particular, there have been many computations of f_B and several of B_B . Thus the lattice provides an alternate way to determine R_1 . But of course it is necessary to know the error in these determinations. One of the systematic errors still present in most lattice calculations is that which arises from the use of the quenched (or valence) approximation, in which disconnected quark loops are neglected. Quenching alters both the short and long-distance properties¹ of the theory. The short-distance effects can, in general, be accounted for by appropriately adjusting the couplings of the theory, but the long-distance effects are more elusive. In a previous paper (5), these effects were studied in heavy-light mesons by extending quenched ChPT[6, 7, 8, 9] to include heavy mesons at leading order in $1/M$. It was found that quenching has a relatively minor effect on B_B and the Isgur-Wise function $\xi(w)$, but a more pronounced effect on f_B . However, the argument in the preceding paragraph suggests that the long-distance effects of quenching should largely be independent of the heavy quark mass. Thus, one might expect that R_1 and similar quantities will be relatively immune to the effects of quenching.

In this paper we will attempt to study this supposition in more detail. Our tool will again be quenched ChPT. Building on the work of BG, we will extend this to include $1/M$ corrections and use it to examine the $1/M$ dependence of the quenched corrections. By comparing these corrections to those found in unquenched ChPT by BG, one obtains an estimate of the error due to the use of the quenched approximation. Of course, the conclusions drawn from this approach are only reliable to the extent that ChPT accurately describes the unquenched physics. The remainder of this paper

¹ Here long and short distances are defined relative to the QCD scale.

is organized as follows. In section 2, we briefly review quenched ChPT for heavy mesons. In section 3, we compute loop corrections to the heavy meson decay constants. In section 4 these results are investigated numerically. In section 5 we conclude. An appendix collects some results on the one-loop counter-terms. For the sake of brevity, we will follow the notation of BG as much as possible and refer the reader to their paper for omitted details.

2 Quenched Chiral Perturbation Theory and the Inclusion of Heavy Mesons

Quenched chiral perturbation theory has been developed in refs. 6, 9 and the extension to heavy mesons fields has recently been discussed in Ref. 5. Consequently we will restrict the presentation here to only that which is necessary to fix notation.

One way to implement quenching[10] is to introduce bosonic “ghost” quarks to cancel the functional determinant which arises from the integral over the fermion fields. The inclusion of these extra particles enlarges the symmetry of the theory. Thus, quenched ChPT is obtained from ordinary unquenched ChPT by enlarging the symmetry group $SU(3)_L \times SU(3)_R$ to the semi-direct product $(SU(3|3)_L \times SU(3|3)_R) \otimes U(1)$. Elements of the graded symmetry group are represented by supermatrices (in block form)

$$U = \begin{pmatrix} A & B \\ C & D \end{pmatrix}, \quad (4)$$

where A and D are matrices composed of even (commuting) elements and B and C are composed of odd (anti-commuting) elements. Group invariants are formed using the super trace str and super determinant $sdet$, defined as

$$str(U) = tr(A) - tr(D), \quad (5)$$

$$sdet(U) = \exp(str \log(U)) = \det(A - BD^{-1}C) / \det(D). \quad (6)$$

To accommodate the larger symmetry, the meson matrix is extended to a supermatrix:

$$\Phi = \begin{pmatrix} \phi & \chi^\dagger \\ \chi & \tilde{\phi} \end{pmatrix}, \quad (7)$$

where $\chi^\dagger \sim \bar{q}q$, $\chi \sim q\bar{q}$ and $\tilde{\phi} \sim \bar{q}q$ and ϕ is ordinary meson matrix

$$\phi = \begin{pmatrix} \frac{1}{\sqrt{2}}\pi^0 + \frac{1}{\sqrt{6}}\eta & \pi^+ & K^+ \\ \pi^- & -\frac{1}{\sqrt{2}}\pi^0 + \frac{1}{\sqrt{6}}\eta & K^0 \\ K^- & \bar{K}^0 & -\sqrt{\frac{2}{3}}\eta \end{pmatrix}. \quad (8)$$

Note that χ and χ^\dagger are fermionic fields, while ϕ and $\tilde{\phi}$ are bosonic.

The Lagrangian of quenched ChPT is given by

$$\mathcal{L}_{Q\chi} = \frac{f^2}{8} [str(\partial_\mu \Sigma \partial^\mu \Sigma^\dagger) + 4\mu_0 str(\mathcal{M}_+)] + \frac{\alpha_0}{2} \partial_\mu \Phi_0 \partial^\mu \Phi_0 - \frac{m_0^2}{2} \Phi_0^2. \quad (9)$$

Here $\Sigma = \xi^2$, $\xi = e^{i\Phi(x)/f}$ (the normalization is such that $f_\pi = 128$ MeV) while

$$\Phi_0 = \frac{1}{\sqrt{3}} str \Phi = \frac{1}{\sqrt{2}}(\eta' - \tilde{\eta}'), \quad (10)$$

$$\mathcal{M} = \begin{pmatrix} M & 0 \\ 0 & M \end{pmatrix}, \quad (11)$$

$$M = \begin{pmatrix} m_u & & \\ & m_d & \\ & & m_s \end{pmatrix}, \quad (12)$$

and $\mathcal{M}_\pm = \frac{1}{2}(\xi^\dagger \mathcal{M} \xi^\dagger \pm \xi \mathcal{M} \xi)$. The chief difference between the quenched and unquenched theories is the presence of the terms involving Φ_0 . In the unquenched theory they can be neglected because they describe the dynamics of the η' meson, which decouples from the theory. But quenching prevents the η' from becoming heavy and decoupling, so these terms must be retained in quenched ChPT.

The propagators that are derived from this Lagrangian are the ordinary ones, except for the flavor-neutral mesons, where the non-decoupling of Φ_0 leads to a curious double-pole structure. It is convenient to adopt a basis U_a for the those mesons corresponding to $u\bar{u}, d\bar{d}$ and so on, including the ghost quark counterparts. Then the propagator takes the form

$$G_{ij} = \frac{\delta_{ij}\epsilon_i}{p^2 - M_i^2} + \frac{(-\alpha_0 p^2 + m_0^2)/3}{(p^2 - M_i^2)(p^2 - M_j^2)} \quad (13)$$

where $\epsilon = (1, 1, 1, -1, -1, -1)$ and $M_i^2 = 2\mu_0 m_i$. It is conventional to treat the second term in the propagator as a new vertex, the so-called hairpin, with the rule that it can be inserted only once on a given line. Large N_c arguments suggest that the kinetic coupling α_0 is small; this is supported by an analysis of $\eta - \eta'$ mixing. Consequently, we follow the usual practice and set it to zero in the sequel.

In heavy quark effective theory[11, 12, 13] the B and B^* fields (for convenience we refer to all heavy mesons as B 's) are grouped into the 4×4 matrix H_a which conveniently encodes the heavy quark spin symmetry:

$$H_a = \frac{1}{2}(1 + \not{v})(\overline{B}_a^{*\mu} \gamma_\mu - \overline{B}_a \gamma_5), \quad (14)$$

$$\overline{H}_a = \gamma^0 H_a^\dagger \gamma^0. \quad (15)$$

Here v^μ is the four-velocity of the heavy meson, the index a runs over the light quark flavors, u, d, s and the subscript "D" indicates that the trace is taken only over Dirac indices. Henceforth we will drop explicit reference to the heavy meson velocity. The quenched heavy mesons can be incorporated into this framework by adding to H extra fields \tilde{B} and \tilde{B}^* derived from the heavy fields B and B^* by replacing the light quark with a ghost quark, so that a also runs over the ghost flavors.

BG (see also Ref. 14) have given the chiral heavy quark Lagrangian to order $1/M$ (throughout the paper M will refer to the spin-averaged meson mass, $M = \frac{1}{4}(M_B + 3M_{B^*})$). To formulate the quenched version one must also include in the Lagrangian vertices which couple Φ_0 to H . Symmetry requires that this coupling occur through $\text{str}(A_\mu)$, which no longer vanishes. Adding these vertices and some extra counter-terms, but including only those terms which actually contribute at $O(1/M)$, one finds

$$\begin{aligned} \mathcal{L} = & -(1 + \frac{\epsilon_1}{M}) \text{tr}_D [\overline{H}_a i \not{v} \cdot D_{ba} H_b] + \frac{\epsilon_2}{M} \text{tr}_D [\overline{H}_a \sigma^{\mu\nu} v \cdot D_{ba} H_b \sigma_{\mu\nu}] \\ & + (g + \frac{g_1}{M}) \text{tr}_D [\overline{H}_a H_b \not{A}_{ba} \gamma_5] + \frac{g_2}{M} \text{tr}_D [\overline{H}_a \not{A}_{ba} \gamma_5 H_b] \\ & + (\gamma + \frac{\gamma_1}{M}) \text{tr}_D [\overline{H}_a H_a \gamma_\mu \gamma_5] \text{str}(A^\mu) + \frac{\gamma_2}{M} \text{tr}_D [\overline{H}_a \gamma_\mu \gamma_5 H_a] \text{str}(A^\mu) \\ & + \lambda_1 \text{tr}_D [\overline{H}_a H_b] (\mathcal{M}_+)_{ba} + \frac{\lambda_2}{M} \text{tr}_D [\overline{H}_a \sigma^{\mu\nu} H_a \sigma_{\mu\nu}] + \frac{\lambda_3}{M} \text{tr}_D [\overline{H}_a \sigma^{\mu\nu} H_b \sigma_{\mu\nu}] (\mathcal{M}_+)_{ba} \\ & + (k_{10} + \frac{k_{11}}{M}) \text{tr}_D [\overline{H}_a i \not{v} \cdot D_{bc} H_b] (\mathcal{M}_+)_{ca} + \frac{k_3}{M} \text{tr}_D [\overline{H}_a \sigma^{\mu\nu} v \cdot D_{bc} H_b \sigma_{\mu\nu}] (\mathcal{M}_+)_{ca}. \quad (16) \end{aligned}$$

Light mesons enter this Lagrangian through the quantities:

$$\begin{aligned} D_\mu &= \partial_\mu + V_\mu, \\ V_\mu &= \frac{1}{2} (\xi \partial_\mu \xi^\dagger + \xi^\dagger \partial_\mu \xi), \quad (17) \end{aligned}$$

$$A_\mu = \frac{i}{2} (\xi \partial_\mu \xi^\dagger - \xi^\dagger \partial_\mu \xi) = -\frac{1}{f} \partial_\mu \Phi + \mathcal{O}(\Phi^3). \quad (18)$$

The couplings λ_i shift the masses of the heavy mesons: the B^* - B mass splitting Δ is given by $\Delta = -8\lambda_2/M$, while λ_1 produces an $SU(3)$ violating mass shift $\delta_q = 2\lambda_1 m_q$ and λ_3 violates both symmetries (though to the order we are working it only contributes at tree level). Taking these shifts into account the B_q and B_q^* propagators become $\frac{i}{2(v \cdot k + \frac{3}{4}\Delta - \delta_q)}$ and $\frac{-i(g_{\mu\nu} - v_\mu v_\nu)}{2(v \cdot k - \frac{1}{4}\Delta - \delta_q)}$, respectively. The propagators of the ghost mesons are the same as their real counterparts. It is convenient to follow BG in adopting a shorthand notation for the Lagrangian (with the understanding that the propagators are the shifted one):

$$\mathcal{L} = -\text{tr}_D [\overline{H}_a i v \cdot D_{ba} H_b] + \tilde{g}_{\overline{H}H} \text{tr}_D [\overline{H}_a H_b \mathcal{A}_{ba} \gamma_5] + \tilde{\gamma}_{\overline{H}H} \text{tr}_D [\overline{H}_a H_a \gamma_\mu \gamma_5] \text{str}(A^\mu), \quad (19)$$

where

$$\tilde{g} = \begin{cases} \tilde{g}_{B^*} = g + \frac{1}{M}(g_1 + g_2) & \text{for } B^* B^* \text{ coupling,} \\ \tilde{g}_B = g + \frac{1}{M}(g_1 - g_2) & \text{for } B^* B \text{ coupling,} \end{cases} \quad (20)$$

and similarly for $\tilde{\gamma}$. In the sequel it will be useful to introduce two more couplings,

$$\hat{g}_{B^*} = g + \frac{(g_1 + g_2/3)}{M}, \quad \hat{\gamma}_{B^*} = \gamma + \frac{(\gamma_1 + \gamma_2/3)}{M}. \quad (21)$$

All of these couplings should be regarded as shorthand. That is, when performing arithmetic with these couplings, only terms to $O(1/M)$ are to be retained. Finally, we record the expression for the weak current² (again with counter-terms)

$$\begin{aligned} J_a^\mu &= i\alpha \left(1 + \frac{\rho_1}{M}\right) \text{tr}_D [\Gamma^\mu H_b \xi_{ba}^\dagger] + i\alpha \frac{\rho_2}{M} \text{tr}_D [\gamma^\sigma \Gamma^\mu \gamma_\sigma H_b \xi_{ba}^\dagger] + \frac{i\alpha}{2M} \text{tr}_D \left[[\Gamma^\mu, \gamma_\sigma] i D_{cb}^\sigma H_c \xi_{ba}^\dagger \right] \\ &\quad + i\alpha \left(\kappa_{10} + \frac{\kappa_{11}}{M}\right) \text{tr}_D [\Gamma^\mu H_c \xi_{cb}^\dagger] (\mathcal{M}_+)_{ba} + i\alpha \frac{\kappa_3}{M} \text{tr}_D [\gamma^\sigma \Gamma^\mu \gamma_\sigma H_c \xi_{cb}^\dagger] (\mathcal{M}_+)_{ba}, \end{aligned} \quad (22)$$

where $\Gamma^\mu = \gamma^\mu L = \gamma^\mu (1 - \gamma_5)/2$.

3 Loop Corrections

In ChPT, loop corrections generate terms which are non-analytic in the mass parameters of the theory. These terms are uniquely predictions because they cannot be canceled by higher-order counter-terms. The loops also generate divergences and finite terms which are analytic; these are absorbed into the counter-terms. In principle, they can be determined by fitting to experimental data, but due to the paucity of data in the heavy-meson sector, we will at times be forced to simply neglect them and they will not be shown in our formulas. We will later discuss the uncertainty arising from this approximation, but fortunately the error in R_1 , which is our main interest, should be free of counter-terms.

As noted in Ref. 5, the loop structure of the quenched theory is rather odd: the theory splits into three copies of a one-flavor theory, distinguished only by the light quark mass. Because of this, all results for B_d or B_u (henceforth we will refer to these simply as B) mesons apply for B_s mesons after an appropriate relabeling.

The loop integrals encountered are either identical to the I_1 and J of BG, or may be obtained from them by differentiation with respect to m^2 , which will be denoted with a prime. More explicitly,

²Here and in the Lagrangian 16 several terms proportional to $\text{str}(\mathcal{M}_+)$ have been since they do not contribute, but their presence can be inferred from the gaps in the numbering of the coefficients.

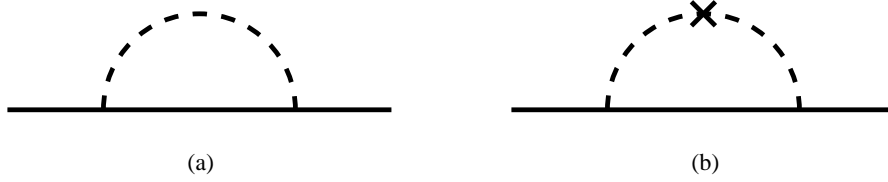


Figure 1: The diagrams which contribute to the heavy meson self energy. Solid lines represent heavy mesons (B , B^*), dashed lines represent light mesons and the cross represents an insertion of the “hairpin” vertex.

we have $J(m, \Delta) = \Delta J_1(m, \Delta)$ and

$$I_1(m) = m^2 \ln(m^2/\mu^2), \quad (23)$$

$$J_1(m, \Delta) = (-m^2 + \frac{2}{3}\Delta^2) \ln(m^2/\mu^2) + \frac{4}{3}(\Delta^2 - m^2)F(m/\Delta), \quad (24)$$

$$F(x) = \begin{cases} \sqrt{1-x^2} \tanh^{-1} \sqrt{1-x^2}, & x \leq 1, \\ -\sqrt{x^2-1} \tan^{-1} \sqrt{x^2-1}, & x \geq 1. \end{cases} \quad (25)$$

The graphs which contribute to the self-energy are shown in Fig. 1. In the diagram of Fig. 1a, the ghost mesons will cancel the contribution from the real mesons unless one of the vertices involves the singlet field. Combining this with the contribution of the hairpin vertex Fig. 1b, we obtain (recall that we are taking α_0 to vanish)

$$i \Sigma_B(v \cdot k) = \frac{6i}{16\pi^2 f^2} \left[2\tilde{g}_B \tilde{\gamma}_B J(M_d, \frac{\Delta}{4} + \delta_d - v \cdot k) + \tilde{g}_B^2 \frac{m_0^2}{3} J'(M_d, \frac{\Delta}{4} + \delta_d - v \cdot k) + \dots \right]. \quad (26)$$

The terms not shown are analytic in M_d and are absorbed in the definition of the counter-terms. For the B^* , we similarly obtain

$$i \Sigma_{B^*}^{\mu\nu}(v \cdot k) = \frac{-2ig^{\mu\nu}}{16\pi^2 f^2} \left[\tilde{g}_B^2 \frac{m_0^2}{3} J'(M_d, \frac{-3\Delta}{4} + \delta_d - v \cdot k) + 2\tilde{g}_{B^*}^2 \frac{m_0^2}{3} J'(M_d, \frac{\Delta}{4} + \delta_d - v \cdot k) \right. \\ \left. + 2\tilde{g}_B \tilde{\gamma}_B J(M_d, \frac{-3\Delta}{4} + \delta_d - v \cdot k) + 4\tilde{g}_{B^*} \tilde{\gamma}_{B^*} J(M_d, \frac{\Delta}{4} + \delta_d - v \cdot k) + \dots \right], \quad (27)$$

where we have neglected a term proportional to $v^\mu v^\nu$. Note that the δ_d dependence will vanish when the on-shell conditions are invoked.

3.1 Wavefunction Renormalization and Decay Constants

The wavefunction renormalization constants are obtained by differentiating the self-energy with respect to $2v \cdot k$ and evaluating on-shell. BG made no assumptions about the magnitude of $\frac{m_\pi}{\Delta}$ and thus retained the function F . In lattice simulations, where both m_π and Δ are adjustable parameters, similar restraint is warranted and so we will also retain F . In terms of the shorthand couplings introduced earlier, the renormalization constants can be written compactly as

$$Z_B = 1 + 3\tilde{g}_B^2 \frac{m_0^2/3}{16\pi^2 f^2} \log \frac{M_d^2}{\mu^2} + 6\tilde{g}_B \tilde{\gamma}_B \frac{M_d^2}{16\pi^2 f^2} \log \frac{M_d^2}{\mu^2} \\ - 6g^2 \frac{m_0^2/3}{16\pi^2 f^2} \frac{\Delta^2 F(\frac{M_d}{\Delta})}{M_d^2 - \Delta^2} - 24g\gamma \frac{\Delta^2}{16\pi^2 f^2} F(\frac{M_d}{\Delta}), \quad (28)$$

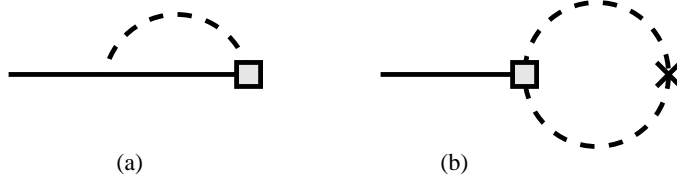


Figure 2: The tadpole correction to the weak current vertex. The box represents an insertion of the weak current.

$$\begin{aligned}
Z_{B^0} = & 1 + 3\hat{g}_{B^*}^2 \frac{m_0^2/3}{16\pi^2 f^2} \log \frac{M_d^2}{\mu^2} + 6\hat{g}_{B^*} \hat{\gamma}_{B^*} \frac{M_d^2}{16\pi^2 f^2} \log \frac{M_d^2}{\mu^2} \\
& - 2g^2 \frac{m_0^2/3}{16\pi^2 f^2} \frac{\Delta^2 F(\frac{M_d}{\Delta})}{M_d^2 - \Delta^2} - 8g\gamma \frac{\Delta^2}{16\pi^2 f^2} F(\frac{M_d}{\Delta}). \quad (29)
\end{aligned}$$

The above expressions have been simplified by discarding terms that are formally of higher order in the chiral and large mass expansions. However, it is important to retain those terms which are needed to make the chiral limit consistent.

Loop corrections to the left-handed current vertex arise from the diagrams of Fig. 2. As was shown by BG, the diagrams of Fig. 2a do not contribute at $O(1/M)$. The remaining tadpole graph Fig. 2b yields for the B

$$\frac{i\alpha v^\mu}{2} \left(1 + \frac{\rho_1 + 2\rho_2}{M}\right) \frac{m_0^2/3}{16\pi^2 f^2} \log \frac{M_d^2}{\mu^2} \quad (30)$$

and for the B^* ,

$$\frac{-i\alpha \epsilon^\mu}{2} \left(1 + \frac{\rho_1 - 2\rho_2}{M}\right) \frac{m_0^2/3}{16\pi^2 f^2} \log \frac{M_d^2}{\mu^2}. \quad (31)$$

The final results for the decay constants are found by combining the wavefunction and vertex corrections:

$$\begin{aligned}
\sqrt{M_B} f_B = & \alpha \left(1 + \frac{\rho_1 + 2\rho_2}{M}\right) \left(1 - \frac{1}{2} \left(1 + 3\hat{g}_B^2\right) \frac{m_0^2/3}{16\pi^2 f^2} \log \frac{M_d^2}{\mu^2} - 3\hat{g}_B \tilde{\gamma}_B \frac{M_d^2}{16\pi^2 f^2} \log \frac{M_d^2}{\mu^2} \right. \\
& \left. + 3g^2 \frac{m_0^2/3}{16\pi^2 f^2} \frac{\Delta^2 F(\frac{M_d}{\Delta})}{M_d^2 - \Delta^2} + 12g\gamma \frac{\Delta^2}{16\pi^2 f^2} F(\frac{M_d}{\Delta})\right), \quad (32)
\end{aligned}$$

$$\begin{aligned}
\frac{1}{\sqrt{M_{B^*}}} f_{B^*} = & \alpha \left(1 + \frac{\rho_1 - 2\rho_2}{M}\right) \left(1 - \frac{1}{2} \left(1 + 3\hat{g}_{B^*}^2\right) \frac{m_0^2/3}{16\pi^2 f^2} \log \frac{M_d^2}{\mu^2} - 3\hat{g}_{B^*} \hat{\gamma}_{B^*} \frac{M_d^2}{16\pi^2 f^2} \log \frac{M_d^2}{\mu^2} \right. \\
& \left. + g^2 \frac{m_0^2/3}{16\pi^2 f^2} \frac{\Delta^2 F(\frac{M_d}{\Delta})}{M_d^2 - \Delta^2} + 4g\gamma \frac{\Delta^2}{16\pi^2 f^2} F(\frac{M_d}{\Delta})\right). \quad (33)
\end{aligned}$$

At this point, let us pause to point out that the nontrivial $1/M$ dependence enters only through the wavefunction renormalization graphs. The tadpole corrections are only multiplicative — they do not see the heavy meson mass. It follows that if the $B^* B \pi$ couplings are weak, the light and heavy quark dependencies of the decay constants will decouple from each other.

To study the size of $1/M$ corrections it is useful to consider the ratio $U(M) = M f_B / f_{B^*}$, which is one in the infinite mass limit. In the quenched theory we find

$$\begin{aligned}
U(M) = & 1 + \frac{4\rho_2}{M} + \frac{4g g_2}{M} \frac{m_0^2/3}{16\pi^2 f^2} \log \frac{M_d^2}{\mu^2} + \frac{4(g\gamma_2 + \gamma g_2)}{M} \frac{M_d^2}{16\pi^2 f^2} \log \frac{M_d^2}{\mu^2} \\
& + 2g^2 \frac{m_0^2/3}{16\pi^2 f^2} \frac{\Delta^2 F(\frac{M_d}{\Delta})}{M_d^2 - \Delta^2} + 8g\gamma \frac{\Delta^2}{16\pi^2 f^2} F(\frac{M_d}{\Delta}), \quad (34)
\end{aligned}$$

while in the full theory

$$\begin{aligned}
U(M) = & 1 + \frac{4\rho_2}{M} + \frac{11}{9} \frac{4gg_2}{M} \frac{m_K^2}{16\pi^2 f^2} \log \frac{m_K^2}{\mu^2} + 8g^2 \frac{\Delta\delta}{16\pi^2 f^2} \log\left(\frac{m_K^2}{\mu^2}\right) \\
& + 6g^2(\Delta + \delta)^2 F\left(\frac{m_K}{\Delta + \delta}\right) - 2g^2(\Delta - \delta)^2 F\left(\frac{m_K}{\Delta - \delta}\right),
\end{aligned} \tag{35}$$

which is easily derived from the work of BG. Here $\delta = \delta_s - \delta_d$ and in order to keep the expression compact we have followed BG in neglecting the pion contribution and approximation $m_\eta^2 = \frac{4}{3}m_K^2$, but the exact expression is used for numeric work.

4 Numeric Results

When studying the error due to quenching, it is interesting to compare our quenched predictions not just with the predictions of BG, but also with the predictions of an unquenched two-flavor theory with degenerate quark masses. Such a theory should describe most unquenched lattice simulations³ and allows one to distinguish between those effects which are due to quenching and those which are due to the simplified flavor structure of the lattice simulations. Results for the two flavor theory can be extracted from the work of BG by taking into account the $SU(3)$ coefficients. In the quenched and two-flavor theories, f_{B_s} is obtained from f_B by substituting $M_s = \sqrt{2m_K^2 - m_\pi^2} = 680$ MeV for M_d . For convenience, the mass of the light mesons in the quenched and two-flavor theories will always be referred to as M_d . Since lattice simulations typically have $M_d > 400$ MeV, it will be useful to study the M_d dependence of our results.

Before proceeding, it is necessary to specify the various couplings which enter the Lagrangian (16). Unfortunately, little information is available. By taking into account chiral loop corrections to strong and radiative D^* decays, one obtains the constraint[15, 16] $0.3 < g + (g_1 - g_2)/M_D < 0.7$, with the central value being slightly less than 0.5. We will choose $g = 0.5$ and $g_1 = g_2$ as our canonical values. QCD sum rules[17, 18, 19, 20] and relativistic quark models[21, 22] favor a smaller value of g , $g \sim 1/3$. They also indicate that $g_1 - g_2$ is small, on the order of 100 MeV, which is roughly consistent with our choice. When necessary, we will assume that both g_1 and g_2 are of this order. This choice is supported by a recent study[23] which found $g_2 \simeq 0.3g$ GeV. A lattice study of heavy meson decay constants by Bernard *et al.*[24] found $\rho_1 + 2\rho_2 = -1.14$ GeV, while a similar study by the UKQCD collaboration[25] found $\rho_1 + 2\rho_2 = -0.8$ GeV. Because the latter group also studied f_{D^*} it is possible to extract ρ_2 from their data; we find $\rho_2 \approx -0.1$ GeV, which is consistent with other determinations[26]. The remaining couplings γ and γ_i are unconstrained. Relative to g and g_i , they are non-leading in $1/N_c$, so they are likely to be small (in the nucleon system, the singlet coupling γ is indeed small[27]). In view of this, we will take $\gamma = \gamma_i = 0$, but it should be kept in mind that this may be an incorrect assumption. The proper choice of m_0 was discussed in Ref. 5; here we choose $m_0 = 750$ MeV.

We begin by considering the ratio R_1 . We first observe that R_1 has only one counter-term, whose contribution is proportional to $(\kappa_{11} + 2\kappa_3)(m_s - m_d)(1/M_D - 1/M_B)$. Since we expect from the nature of the chiral expansion that the counter-terms will be about the same in the quenched and full theories⁴, it follows that the *error* in R_1 will only weakly depend on the counter-term. With this in mind, we neglect it and summarize the results in Table 1.⁵ When the reference values are chosen, $R_1 - 1$ is -0.026 in the full theory, -0.053 in the quenched theory, but $+0.043$ in the two flavor

³A more accurate treatment would take into account the difference between the valence and sea quark masses by using partially quenched ChPT[9]

⁴We do not expect them to be exactly the same because the two theories have different divergences, but they should be close if the lattice is doing a good job of describing QCD

⁵The fact that our result in the three flavor case agrees with that of BG is something of a coincidence, because we have chosen to use $f = f_\pi$ while they use $f = f_K$ and we have also retained the pion contribution.

Table 1: Quenched and unquenched results for R_1 .

Theory	$R_1 - 1$
quenched	$-0.21g^2 + 0.20 \text{ GeV}^{-1}g(g_1 - g_2) + 0.23g\gamma - 0.097 \text{ GeV}^{-1}(g(\gamma_1 - \gamma_2) + \gamma(g_1 - g_2))$
$N_f = 2$	$0.17g^2 - 0.15 \text{ GeV}^{-1}g(g_1 - g_2)$
$N_f = 3$	$-0.10g^2 - 0.14 \text{ GeV}^{-1}g(g_1 - g_2)$

Table 2: Numerical results for R_1 for various models and couplings. The couplings are chosen as follows: Set 1 (BG): $g = 0.75$, $g_1 = g_2$; Set 2: $g = 0.5$, $g_1 = g_2$; Set 3: $g = 0.5$, $g_1 - g_2 = 0.2 \text{ GeV}$; Set 4: $g = 0.5$, $g_1 - g_2 = -0.2 \text{ GeV}$.

Theory	$R_1 - 1$			
	Set 1	Set 2	Set 3	Set 4
quenched	-0.11	-0.052	-0.032	-0.073
$N_f = 2$	+0.087	+0.043	+0.028	+0.058
$N_f = 3$	-0.052	-0.025	-0.040	-0.012

theory. In order to explore the dependence of these results on the couplings, we show in Table 2 the results for several different choices of g and g_i . The first set corresponds to the parameters chosen by BG, the second set is our canonical one, and the next two explore the dependence on $g_1 - g_2$. It can be seen that the error (which is the difference between the full and quenched results) is no more than 6% and not half that for the favored choice of couplings. Thus as hoped quenching has little effect on R_1 — the large tadpole corrections found in Ref. (5) cancel in the ratio and the remaining corrections are small. Interestingly, the results in the two-flavor case suggest that dynamical simulations will do worse than the quenched simulations.

The results for R_1 can be understood by looking at the ratio f_{B_s}/f_B as a function of M . Figure 3 compares the various theories, neglecting counter-terms. The most striking feature is the “kink” in

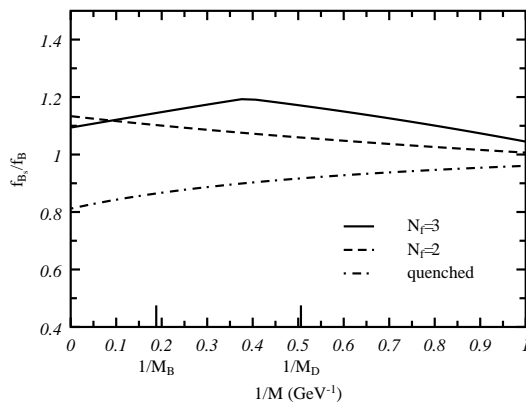


Figure 3: Plot of the ratio f_{B_s}/f_B in the various theories.

the three-flavor case⁶, which occurs when $\Delta = \delta_s$, causing the denominator in the argument of one

⁶ BG presumably did not comment on this kink because their work only required the ratio at the two physical values of M .

of the functions F to vanish (c.f. the expression for $U(M)$ in Eq. (35)). Physically, this corresponds to the case when the B_s and the B^* are degenerate, leading to an enhancement of f_{B_s} . Without this kink, the ratio would be a slowly increasing function of M , just as it is in the two-flavor theory. In a sense, then, the small error in R_1 is a fortunate coincidence. While the details of the curves in Fig. 3 depend on our choice of g and g_i , the shapes are generic. As g increases, or $g_1 - g_2$ becomes negative, the magnitudes of the slopes increases, so that the curves draw together more at small M without changing their shape or relative positions. In particular, there is always a large gap between the quenched and full predictions. Thus a general conclusion of this analysis is that quenching decreases the ratio f_{D_s}/f_D . In addition, the different M dependence predicted by the three theories makes this ratio a test of the chiral description of the decay constants.

We next consider f_B directly. This is primarily for illustrative purposes since the dynamical theories have an extra counter-term proportional to $\text{tr}(M_+)$, making direct comparison to the quenched theory difficult; here we will simply neglect the counter-terms. Figure 4 then shows both $\hat{F}_B = \sqrt{M}f_B/\alpha$ and \hat{F}_{B_s} together with the quenched and two flavor predictions. In the $M \rightarrow \infty$

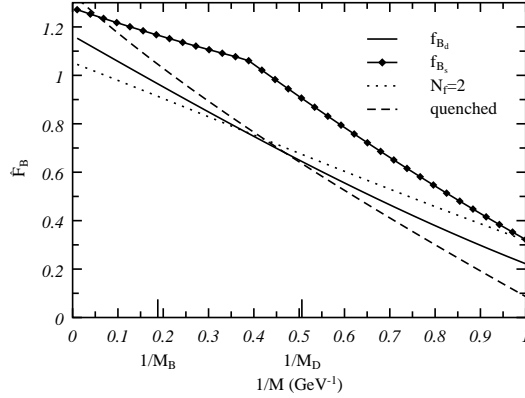


Figure 4: Plot of $\hat{F} = \sqrt{M}f_B/\alpha$ in the various theories, with $M_d = m_\pi$.

limit the results are consistent with those found in Ref. 5. The behavior of f_B is dominated by the tree-level term $(\rho_1 + 2\rho_2)/M$. In Fig. 5, we study the M_d dependence of the error in f_B , comparing both the quenched and two flavor theories to the true theory. In the error, the tree-level terms cancel, making it easier to see the non-trivial M dependence. One sees that the M and m_q depen-

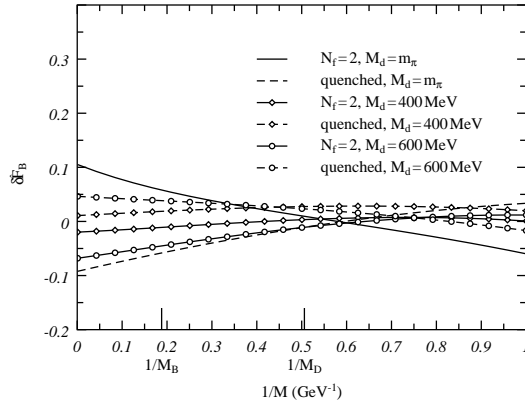


Figure 5: Plot of the differences $\delta\hat{F}_B = \hat{F}_B(\text{quenched}) - \hat{F}_B(\text{full})$ and $\delta\hat{F}_B = \hat{F}_B(N_f = 2) - \hat{F}_B(\text{full})$ for various values of M_d .

dence are closely intertwined, as the both the quenched and two-flavor errors switch sign between $M_d = m_\pi$ and $M_d = 400$ MeV. Even at its largest, the quenched error is no more than 7% in the region between $M = M_B$ and $M = M_D$. Also, observe that except for the smallest value of M_d , the error tends to decrease as M decreases.

Finally, we examine the $1/M$ dependence of f_B through the quantity $U(M)$. Once again there is the problem that the dynamical theories have one more counter-term than the quenched theory. This could be eliminated by considering the ratio $U_s(M)/U_d(M)$, but we will again simply neglect the counter-terms. In Fig. 6 we show U for various values of the light quark mass. For $M_d = m_\pi$,

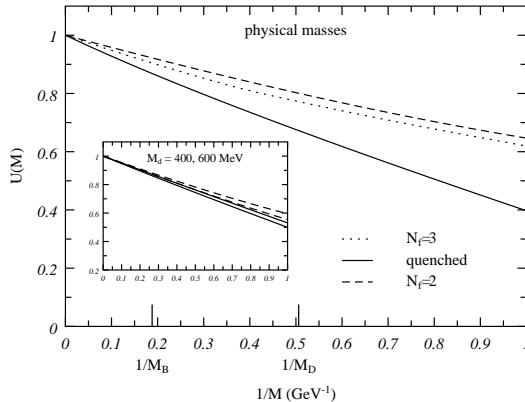


Figure 6: Plot of the ratio $U(M) = M f_B / f_B^*$. The inset graph shows the M_d dependence of the quenched and two-flavor theories. As M_d increases, the curves of two theories approach each other, overlapping near $M_d = M_s$ and then moving apart again.

quenching has a pronounced effect. But for larger values of M_d , there is almost no difference between the quenched and two-flavor theories. Thus lattice simulations are unlikely to observe any effect of quenching in $U(M)$. Note that since all the theories must agree at $M = \infty$, the quenching error can only increase as M decreases.

To conclude our discussion of numeric results, let us comment on the uncertainty arising from the neglect of the counter-terms. In ChPT for the light mesons, the counter-terms are small, close to their natural size of $1/(4\pi)^2$ [28]. Goity[2] has observed that choosing $\mu = 1.5$ GeV effectively mimics the inclusion of these analytic terms. While we do not know whether this works for the heavy mesons, it certainly does generate terms of the natural size. However, it cannot be completely correct for the quenched case because of the different behavior of the quenched logarithms under scaling. Nonetheless, it serves as a useful way to add counter-terms of the expected size.⁷ Doing this, we find that in all the theories R_1 is almost independent of μ , changing by only a few percent. $U(M)$ also changes very little, again only a few percent. f_B and the ratio f_{B_s}/f_B , however, are more strongly effected: typical shifts are 10 – 15%. However, the general features of f_{B_s}/f_B that were observed in Fig. 3 are unchanged.

5 Conclusions

By generalizing quenched ChPT to include heavy mesons and including $1/M$ corrections following Boyd and Grinstein[4], we have studied the $1/M$ dependence of the quenching errors in lattice simulations. We found that unknown counter-terms prevented us from making definitive statements

⁷ A more ambitious approach would be to assume that resonances saturate the counter-terms, as they do in the light-meson sector[28].

about the behavior of f_B , but it was possible to reduce this uncertainty by taking appropriate ratios, such as R_1 . Although the long-distance effects of quenching are not independent of the heavy mass M , they were fairly insensitive to it. As a result, the error in R_1 was found to be small, only a few percent. We saw that f_{B_s}/f_B is smaller in the quenched theory, a result that was observed earlier in the $M \rightarrow \infty$ limit[5]. We also observed an effect not directly related to quenching, but nonetheless missing in lattice simulations, namely the enhancement of f_{B_s} when B_s and B^* are nearly degenerate. This enhancement had a strong impact on R_1 in the full theory. In future work it would be desirable to determine the counter-terms in some way, either from models or directly from lattice data.

Acknowledgements

We would like to thank the University of Chicago theory group for its hospitality while this work was initiated. This work was supported in part by DOE grant DE-FG05-86ER-40272.

A Renormalized Couplings

Within the context of dimensional regularization, the singularities of the effective Lagrangian are conventionally described in terms of the parameter $L(\mu)$ which contains the singularity at $D = 4$ ($\epsilon = 2 - D/2$, $1/\hat{\epsilon} = 1/\epsilon + \log 4\pi + 1 - \gamma_E$):

$$L(\mu) = \frac{1}{16\pi^2} \mu^{-2\epsilon} \frac{1}{\hat{\epsilon}}. \quad (\text{A.1})$$

With the convention that an arbitrary coupling k is written as $k = k^r(\mu) + \bar{k} L(\mu)$, the following choices render the Lagrangian Eq. (16) finite.

$$\bar{k}_{10} = 6g\gamma \frac{2\mu_0}{f^2} \quad (\text{A.2})$$

$$\bar{k}_{11} = 6(g\gamma_1 + g_1\gamma) \frac{2\mu_0}{f^2} \quad (\text{A.3})$$

$$\bar{k}_3 = (g\gamma_2 + g_2\gamma) \frac{2\mu_0}{f^2} \quad (\text{A.4})$$

$$\bar{\epsilon}_1 = 2g g_1 \frac{m_0^2/3}{f^2} \quad (\text{A.5})$$

$$\bar{\epsilon}_2 = -2g g_2 \frac{m_0^2/3}{f^2} \quad (\text{A.6})$$

In addition, it is necessary to add the counter-term

$$3g^2 \frac{m_0^2/3}{f^2} \text{tr}_D [\bar{H}_a i v \cdot D_{ba} H_b]. \quad (\text{A.7})$$

The current Eq. (22) is renormalized with the choices

$$\begin{aligned} \bar{\rho}_1 &= \left[\frac{1}{2}(1 + 3g^2)\rho_1 + g(3g_1 - g_2) \right] \frac{m_0^2/3}{f^2}, \\ \bar{\rho}_2 &= \left[\frac{1}{2}(1 + 3g^2)\rho_2 + gg_2 \right] \frac{m_0^2/3}{f^2}, \\ \bar{\kappa}_{10} &= 6g\gamma \frac{\mu_0}{f^2}, \end{aligned}$$

$$\begin{aligned}
\bar{\kappa}_{11} &= [g(3\gamma_1 - \gamma_2) + \gamma(3g_1 - g_2)] \frac{2\mu_0}{f^2}, \\
\bar{\kappa}_3 &= (g\gamma_2 + \gamma g_2) \frac{2\mu_0}{f^2},
\end{aligned}
\tag{A.8}$$

and it is also necessary to rescale α :

$$\alpha^r(\mu) = \alpha \left[1 + \frac{1}{2}(1 + 3g^2) \frac{m_0^2/3}{f^2} L(\mu) \right].
\tag{A.9}$$

Finally, the mass terms in the Lagrangian must also be shifted

$$\begin{aligned}
\bar{\lambda}_3 &= 16g\gamma\lambda_2 \frac{2\mu_0}{f^2}, \\
\bar{\lambda}_2 &= 8g^2 \frac{m_0^2/3}{f^2}.
\end{aligned}
\tag{A.10}$$

References

1. B. Grinstein *et al.*, Nucl. Phys. **B380**, 369 (1992).
2. J. L. Goity, Phys. Rev. D **46**, 3929 (1992).
3. B. Grinstein, Phys. Rev. Lett. **71**, 3067 (1993).
4. C. G. Boyd and B. Grinstein, preprint UCSD-PTH-93-46 (hep-ph/9402340).
5. M. J. Booth, preprint IFT-94-09.
6. C. W. Bernard and M. F. Golterman, Phys. Rev. D **46**, 853 (1992).
7. S. R. Sharpe, Phys. Rev. D **41**, 3233 (1990).
8. S. R. Sharpe, Phys. Rev. D **46**, 3146 (1992).
9. C. W. Bernard and M. F. Golterman, Phys. Rev. D **49**, 486 (1994).
10. A. Morel, J. Physique **48**, 111 (1987).
11. M. Wise, Phys. Rev. D **45**, 2188 (1992).
12. G. Burdman and J. F. Donoghue, Phys. Lett. B **280**, 287 (1992).
13. T.-M. Yan *et al.*, Phys. Rev. D **46**, 1148 (1992).
14. N. Kitazawa and T. Kurimoto, Phys. Lett. B **323**, 65 (1994).
15. J. F. Amundson *et al.*, Phys. Lett. B **296**, 415 (1992).
16. H.-Y. Cheng *et al.*, Phys. Rev. D **49**, 5857 (1994).
17. V. M. Belyaev, V. M. Braun, A. Khodjamirian, and R. Ruckl, preprint MPI-PhT/94-62 (hep-ph/9410280).
18. P. Colangelo *et al.*, preprint UGVA-DPT 1994/06-856 (hep-ph/9406295).
19. A. Grozin and O. I. Yakovlev, preprint BUDKERINP-94-3 (hep-ph/9401267).
20. V. L. Eletsky and Y. I. Kogan, Z. Phys. **28**, 155 (1985).
21. P. Colangelo, F. D. Fazio, and G. Nardulli, Phys. Lett. B **334**, 175 (1994).
22. M. Sutherland, B. Holdom, S. Jaimungal, and R. Lewis, preprint UTPT-94-25 (hep-ph/9410324).
23. N. D. Bartolomeo, R. Gatto, F. Feruglio, and G. Nardulli, preprint UGVA-DPT 1994/10-864 (hep-ph/9411210).
24. C. W. Bernard, J. N. Labrenz, and A. Soni, Phys. Rev. D **49**, 2536 (1994).
25. R. M. Baxter *et al.* (UKQCD Collaboration), Phys. Rev. D **49**, 1594 (1994).
26. R. Sommer, preprint DESY-94-011 (hep-lat/9401037).
27. T. Hatsuda, Nucl. Phys. **B329**, 376 (1990).
28. G. Ecker, J. Gasser, A. Pich, and E. de Rafael, Nucl. Phys. **B321**, 311 (1989).